ELSEVIER

Urologic Oncology: Seminars and Original Investigations 000 (2022) 1−8

UROLOGIC ONCOLOGY

Clinical-Prostate cancer

A magnetic resonance imaging-based nomogram for predicting clinically significant prostate cancer at radical prostatectomy

Daniele Castellani, MD[a,1,*], Sara Cecchini, MD[b,1], Roberta Mazzucchelli, MD[c], Luca Soraci, MD[d], Mirko Di Rosa, PhD[e], Paolo Fabbietti, MS[e], Erika Palagonia, MD[a], Francesca Puccio, MD[f], Francesca Carnevali, MD[b], Enrico Paci, MD[b], Rodolfo Montironi[c], Andrea Benedetto Galosi[a]

[a] *Unit of Urology, Polytechnic University of the Marche Region, Azienda Ospedaliero-Universitaria Ospedali Riuniti di Ancona, Ancona, Italy*
[b] *Unit of Radiology, IRCSS INRCA, Ancona, Italy*
[c] *Section of Pathological Anatomy, Polytechnic University of the Marche Region, School of Medicine, Azienda Ospedaliero-Universitaria Ospedali Riuniti di Ancona, Ancona, Italy*
[d] *Unit of Geriatric Medicine, IRCSS INRCA, Cosenza, Italy*
[e] *Unit of Geriatric Pharmacoepidemiology and Biostatistics, IRCCS INRCA, Ancona, Italy*
[f] *Unit of Pathology and Cytopathology, Azienda Ospedaliero-Universitaria Federico II, Napoli, Italy*

Received 17 October 2021; received in revised form 28 February 2022; accepted 18 April 2022

Abstract

Purpose: To develop a nomogram incorporating clinical and multiparametric magnetic resonance imaging (mpMRI) parameters for the detection of clinically significant prostate cancer (csCaP) at radical prostatectomy (RP).

Materials and Methods: We retrospectively analyzed all consecutive patients who underwent robotic RP between 2016 and 2020. All patients underwent a 1.5-T mp-MRI according to the PI-RADS-v2 scoring system. RP specimens were examined with the whole-mount technique. csCaP definition: any tumor with a volume larger than 0.5 cm^3 or with a Gleason score ≥7. Univariable logistic regression models explored the association between clinical and imaging data and the risk of csCaP. Significant variables ($P < 0.05$) were selected into multivariable regression models to identify independent predictors. A nomogram was designed to select the significant relevant predictors. The nomogram was internally validated in terms of discrimination and calibration. Receiver operating characteristics of the area under the curve was used to assess the discrimination ability of the nomogram. To assess the predictive performance of mpMRI, the accuracy of the mpMRI-based nomogram was compared with that excluding either PI-RADS score or mpMRI IL size.

Results: The analysis involved 393 patients. The median age was 65(9) years. The median prostate specific antigen was 5.81(3.76) ng/ml. 363 had csCaP. PI-RADS v2 score of 4-5, prostate specific antigen density of 0.15 or more, and mpMRI index lesion (IL) size were significantly associated with csCaP in the multivariable regression analyses. Based on these variables, a diagnostic model was developed. The full model yielded an area under the curve of 0.77 (95%CI:0.75−0.80) which was significantly better than those excluding mpMRI findings ($P = 0.02$) Decision curve analysis showed a slight but significant net benefit associated with the use of the mp-MRI based nomograms compared with those excluding either PI-RADS score (Delta net benefit 0.0278) or mpMRI maximum IL size (Delta net benefit 0.0111).

Conclusions: The nomogram constructed in this study can assist urologists in assessing an individual's risk of csCaP at RP.

Keywords: Nomograms; Multiparametric magnetic resonance imaging; Prostatic neoplasms

1. Introduction

The role of multiparametric magnetic resonance imaging (mpMRI) in the pathway for the diagnosis of prostate cancer (CaP) has been rapidly evolved over the last decade.

[1]Daniele Castellani and Sara Cecchini equally contributed to the paper.

*Corresponding author. Tel.: +39-3-471814691; fax: +39-7-15963367.
E-mail address: castellanidaniele@gmail.com (D. Castellani).

https://doi.org/10.1016/j.urolonc.2022.04.011
1078-1439/

mpMRI was originally employed to improve the detection of CaP in men with prior negative biopsies and elevated prostate specific antigen (PSA) levels [1]. More recently, the PROMIS trial showed that upfront mpMRI, to triage men with suspicious CaP, allowed 27% of patients to avoid a primary biopsy and reduced the diagnosis of clinically insignificant cancers by 5% when compared with the standard pathway of prostate biopsy [2]. Moreover, the PRECISION trial confirmed that fewer men in the MRI-targeted biopsy group received a diagnosis of non- csCaP than in the standard-biopsy group [3]. A recent meta-analysis on 48 studies including 9613 patients showed that the median negative predictive value of mpMRI was 82.4% (IQR, 69% −92.4%) for overall cancer and 88.1% (IQR, 85.7% −92.3%) for clinically significant csCaP [4].

The current European Association of Urology guidelines emphasize individual risk assessment and underline the potential role of CaP risk calculators in enhancing mpMRI performance [5]. mpMRI was recently incorporated into risk calculators with clinical parameters for determining the risk of having csCaP for individualized pre-biopsy risk assessment [6–9]. However, risk calculators incorporating mpMRI and predicting csCaP at radical prostatectomy (RP) are lacking. The present study aimed to develop a predictive model and nomogram that incorporates clinical data and mpMRI parameters for the detection of clinically significant CaP (csCaP) at RP.

2. Materials and methods

2.1. Study design and participants

This study is a retrospective analysis of all consecutive patients who underwent robotic RP with or without pelvic lymph node dissection for CaP in our center between 2016 and 2020. Inclusion criteria were adenocarcinoma histotype and a mpMRI performed before prostate biopsy or surgery (local staging intent). Exclusion criteria were previous and/or concomitant treatment of CaP and the unavailability of a mpMRI study. Patients with missing data were also excluded. The study was approved by our local Ethical Board (DGEN 278/2019). All patients signed an informed consent form.

2.2. mp-MRI protocol

All patients underwent a 1.5-T mp-MRI study with a 32-channel surface coil (Ingenia, Philips, Milan, Italy). MRI was performed before biopsy (targeted biopsy) or 6 weeks after biopsy for local staging. In accordance with the European Society of Urogenital Guidelines [10], the acquisition protocol consisted of multiplanar T2-weighted images, diffusion-weighted imaging (with a b-value of 0-800-1400-1600-2000 s/mm2 including the calculation of apparent diffusion coefficient maps), dynamic gadolinium contrast-enhanced imaging sequences, and T1-weighted images with a large field-of-view. mp-MRI was performed at least 4 weeks after prostate biopsy. Two dedicated radiologists analyzed the images and were blinded to the histopathology report. Images were scored in line with the Prostate Imaging-Reporting and Data System (PI-RADS) v2 assessment categories [10]. Age, body mass index, PSA, prostate volume at mp-MRI, PSA density, and the numbers and the largest diameter of the index lesion at mp-MRI were gathered. The MRI-index lesion was defined as the lesion with the highest PI-RADS v2 score or the largest lesion in the presence of more than 1 lesion with the same score.

2.3. Assessment of RP specimens

All samples were analyzed by 2 experienced uropathologists. RP specimens were embedded and examined with the whole-mount technique [11]. Each specimen was received fresh from the operating room. To enhance a quick and uniform fixation, 100 mL of 10% buffered formalin was introduced into the prostate at multiple sites using a fine hypodermic needle. The specimen was then covered with India ink and fixed for 24 hours in formalin. After fixation, the sectioning procedure was employed for each specimen. Seminal vesicles were removed from the prostate and cut into 2 halves [12]. The apical and basal parts of the prostate were removed by a transversal cut at 4 mm from the distal and proximal margins, respectively, and then sectioned into slices at 4 mm intervals perpendicularly to the inked surface. The prostate body was step-sectioned at 4 mm intervals, perpendicular to the gland's long axis (apical-basal). The cut specimen was post-fixed for 24 hours in formalin and then dehydrated in graded alcohols, cleared in xylene, embedded in paraffin, and examined histologically as 5 μm-thick whole-mount hematoxylin and eosin-stained sections. For the body of the prostate, sections were used with special molding and inclusion cassettes. The slides were at least 76 mm long and 50 mm wide. We used a stereological method in each specimen, using point counting based on overlaid grids to calculate the total volume of cancer and the volume of the major focus of prostate cancer [13]. Cancer foci were identified in each section, which we delimited by pen dots. The number of grid points falling within the cancer area was then counted. The value of the area associated with each grid point was multiplied by the thickness of the slice (4 mm). This gave the volume of cancer in a prostate slice. The volume obtained in all slices was added up and then multiplied by a shrinking factor of 1.3, giving the volume of cancer in cc. The 2014 International Society of Urological Pathology modified Gleason score and Grade Group were provided [14]. csCaP was defined as any tumor with a volume larger than 0.5 cm^3 or with a Gleason score ≥7 [15]. The index lesion was considered as the cancer focus with the highest Gleason score, or the largest focus as measured by the volume in the case of more than 1 lesion with the same Gleason score [16]. The index lesion volume, pT, grading group, extraprostatic extension (yes/no), positive surgical margins (yes/no), and metastatic lymph nodes (yes/no) were gathered.

2.4. Statistical analysis

Descriptive statistics of the study population were calculated according to the occurrence of csCaP . Continuous variables were reported as median and interquartile range (IQR) and compared by using a Mann-Whitney U test. Categorical variables were reported as numbers and percentages and tested with a chi-square test. Univariable logistic regression models were carried out to explore the association between clinical and imaging data and the risk of csCaP. Variables with a *P*-value <0.05 in univariate analysis were then selected into multivariable regression models to identify independent predictors. Multivariate logistic regression coefficients were used to develop the multivariable nomograms that predict the probability of csCaP. The variance inflation factor (VIF) was additionally measured in the multivariable logistic regression analysis to investigate the degree of multicollinearity among covariates, and VIF >10 was used to define the presence of high multicollinearity [17]. According to the results of the multivariable logistic regression analysis, a nomogram was designed to select the significant relevant predictors using a backward step-down process using the Akaike information criterion [18]. The internal validation of the nomogram was evaluated in terms of discrimination and calibration. Discrimination performance was numerically assessed by calculating Harrell's concordance index (C-index) [19]. Fractional polynomials were used to determine the appropriate functional form for continuous variables [20]. Furthermore, receiver operating characteristics of the AUC were used to compare the nomogram's discrimination ability with that of single linear predictors, and predictive accuracy was expressed in terms of the AUC value. Additionally, the predictive accuracy of mpMRI was assessed by comparing the performance of predictive models with and without mpMRI IL size and those with and without PI-RADS score.

Secondly, calibration was evaluated by plotting the relationship between actual probability and predicted probabilities using a bootstrapping method with 1,000 replications. To account for the nomogram's clinical usability, decision curve analysis (DCA) was conducted by computing the net benefits for a range of threshold probabilities [21]. DCA performance was expressed in terms of delta net benefit derived as the difference between the net benefit of the full model and that of the 'Treat All' approach. To account for differences between distinct decision curve analyses, we compared the net benefit of DCA including PI-RADS, maximum MRI IL size, and PSA density with that of the models excluding either PI-RADS or IL size. Statistical analyses were performed using "pROC," "rms," "rmda," and "survival" packages in R version 4.1.0 (R Foundation, https://www.r-project.org) [22,23]. A 2-sided *P*-value with a threshold of 0.05 was used to determine statistical significance.

3. Results

Five hundred and seventeen men underwent RP during the study period. Among them, 393 patients met the inclusion criteria and were included in the analysis. Table 1 shows the patients' characteristics. The median age was 65 (9) years, while the median PSA was 5.81(3.76) ng/ml. The median prostate volume was 37.75(21.97) cc. On pathologic findings at needle biopsy, 61 patients had non csCaP, based on Epstein's criteria (Gleason score 6 and <3 cores with cancer or ≤ 50% of core involved by cancer) [24]. However, they refused active surveillance and opted for RP. Based on pathological findings at RP, 363 had csCaP. The median PSA was significantly higher in patients with csCaP compared to patients with non-csCaP [5.93(3.77) vs. 4.80(3.87) ng/ml, respectively, $P = 0.034$]. Median PSA density was higher in patients with csCaP [0.152(0.114) vs. 0.093(0.076) ng/ml/cc respectively, $P < 0.001$]. Concerning mpMRI findings, the incidence of PI-RADS lesions significantly differed between patients with clinically significant and non-csCaP ($P < 0.001$). The PI-RADS score ≤3 was present in 12 of 30 (40%) patients with non-csCaP and 41 of 363 (11.3%) patients with csCaP. Conversely, the PI-RADS score 5 was seen in 122 of 363 (33.6%) csCaP patients, whilst only 2 of 30 (6.7%) non-csCaP patients had a score 5 lesion.

In the multivariate analysis, PSA density of 0.15 ng/ml or more, PI-RADS score 4-5, and the maximum length of the mpMRI IL were independent risk predictors for the presence of csCaP (Table 2).

A diagnostic model was developed, which included PI-RADS score, PSA density, and the maximum length of the mpMRI IL for predicting csCaP at RP. The model yielded an AUC of 0.77 (95%CI: 0.75−0.80) (Fig. 1A), which was significantly better compared to that of the model without PI-RADS score (AUC 0.75, 0.68−0.78, $P = 0.02$) and mpMRI IL size (AUC 0.73, 0.69− 0.75, $P = 0.002$). The calibration curve showed good consistency between the predicted probability of the model and the actual probability of csCaP (Fig. 1B). The DCA did not show a significant net benefit (NB) of the full model including PI-RADS, mpMRI IL size, and PSA density compared to the "Treat All" approach at clinically plausible thresholds; indeed, improvement in net benefit was visible for risk thresholds over 53%, significant over 60% and more evident when RT reaches 80%. However, the DCA net benefit of the model including PI-RADS, maximum MRI IL size, and PSA density was slightly better than those excluding either IL size (Delta net benefit of 0.0111) or PI-RADS (Delta net benefit of 0.0278) at a 50% RT (Fig. 2A and B) and significantly increases at 60% RTs. After 1,000 bootstrap resamples, a regression coefficient-based nomogram predicting the probability of csCaP at RP was developed from the full model (Fig. 3).

Table 1
Descriptive statistics of patients included in the study

	Total $n = 393$	Clinically significant $n = 363$	Nonclinically significant $n = 30$	P
Age (y), median(IQR)	65 (9)	65 (10)	64 (8.2)	0.175
BMI, median(IQR)	25.76 (4.50)	25.80	25.11	0.431
PSA (ng/ml), median(IQR)	5.81 (3.76)	5.93 (3.77)	4.80 (3.87)	0.034
Prostate volume (cc), median (IQR)	37.75 (21.97)	37.00 (20)	50.35 (23)	<0.001
PSA density (ng/ml/cc), median (IQR)	0.146 (0.11)	0.152 (0.114)	0.093 (0.076)	<0.001
PSA density ≥ 0.15 ng/ml/cc, *n*(%)	193 (49.3)	189 (52.1)	4 (13.3)	<0.001
PI-RADS score, *n* (%)				<0.001
1-3	53 (13.5)	41 (11.3)	12 (40.0)	
4-5	340 (86.5)	322 (88.7)	18 (60.0)	
Maximum MRI IL size (mm), median (IQR)				
	12 (7)	12 (7)	10 (9)	0.003
Radical prostatectomy IL volume (cc), median (IQR)				
	1.086 (1.453)	1.211 (1.49)	0.22 (0.2)	<0.001
Grading Group at radical prostatectomy, *n* (%)				<0.001
1	58 (14.8)	28 (7.7)	30 (100)	
2	221 (56.2)	221 (60.9)		
3	84 (21.4)	84 (23.1)		
4	9 (2.3)	9 (2.5)		
5	21 (5.3)	21 (5.8)		
pT, *n* (%)				<0.001
2	230 (58.5)	200 (55.1)	30(100)	
3a	129 (32.8)	129 (35.5)		
3b	25 (6.4)	25 (6.9)		
4	9 (2.3)	9 (2.5)		
Extraprostatic extension, *n* (%)				
No	230 (58.5)	200 (55.1)	30 (100)	<0.001
Yes	163 (41.5)	163 (44.9)		
Positive surgical margin, *n*(%)				
No	268 (68.2)	240 (66.1)	28 (93.3)	0.002
Yes	125 (31.8)	123 (33.9)	2 (7.7)	
Lymphadenectomy, *n*(%)				
Not performed	155 (39.4)	138 (38.0)	18 (60.0)	0.131
Metastatic	33 (8.4)	31 (8.5)	0 (0)	
Negative				
	205 (52.2)	194 (53.4)	12 (40.0)	

BMI = body mass index; IL = index lesion. IQR = interquartile range; MRI = magnetic resonance imaging; PI-RADS = Prostate Imaging Reporting and Data System; PSA = prostate specific antigen.

Notes: *P*-value from $\chi 2$ test or Mann-Whitney U test as appropriate.

4. Discussion

Several prediction calculators have been introduced in clinical practice to assist urologists in selecting patients with suspicious CaP for biopsy. However, the most commonly-used calculators only include clinical data, without using mpMRI. The European Randomized Study of Screening for Prostate Cancer derived Prostate Risk Calculator was developed using a model for the risk of high-grade disease (Gleason score ≥7) associated with age at biopsy, race, family history of prostate cancer, PSA level, PSA velocity, digital rectal examination, and previous prostate biopsy [25]. This model showed an AUC performance of 0.68. Similarly, the North American Prostate Cancer Prevention Trials based Cancer Risk Calculator showed an AUC of 0.72 adopting PSA, digital rectal examination, prostate volume, and transrectal ultrasound results [26]. The introduction of mpMRI into screening programs reduced the risk of overdiagnosis of insignificant CaP, with a reported pooled sensitivity of 84% and specificity of 75% for csCaP with a PI-RADS threshold of 3 or 4 [27]. As a consequence, risk calculators incorporating MRI findings have recently been introduced into the diagnostic pathway for patients with suspicious CaP, showing more powerful risk stratification than the previous multivariable prediction nomograms. The European Randomized Study of Screening for Prostate Cancer derived Prostate Risk Calculator was recently improved by incorporating age and mpMRI, showing an AUC 0.84 and 0.85 in biopsy naïve and previously biopsied men, respectively [9]. van Leeuwen et al. developed a model based on a prospective series of 393 men who underwent mpMRI before prostate biopsy, incorporating age, PSA, digital rectal examination, previous biopsy, prostate volume, and the mpMRI PI-RADS score [6]. The authors found that the AUC of their model for

Table 2
Logistic regression models exploring association between selected study risk factors and clinically significant prostate cancer

Sample (n =393)	Univariate logistic regression model OR (95%CI)	P	Multivariate logistic regression model OR (95%CI)	P
Age	1.03 (0.97−1.08)	0.39	1.01 (0.96−1.05)	0.75
PSA density ≥0.15 ng/ml	7.06 (2.68−24.29)	<0.001	5.64 (2.09−19.69)	0.002
PI-RADS score 4−5	5.24 (2.31−11.57)	<0.001	2.90 (1.09−7.47)	0.03
Maximum MRI IL size	1.15 (1.07−1.24)	<0.001	1.07 (1.01−1.17)	0.04

IL = index lesion. MRI = Magnetic Resonance Imaging; PSA = prostate specific antigen. PIRADS = Prostate Imaging Reporting and Data System.
IL = Index Lesion. OR = Odds Ratio. CI = confidence interval.

predicting csCaP at needle biopsy (Gleason 7 with >5% grade 4, ≥20% cores positive or ≥7 mm of cancer in any core) was 0.864 after external validation, reducing 28% of biopsies, whilst missing 2.6% of csCaP. Bjurlin et al. developed another nomogram incorporating PSA density, age, and PI-RADS score lesions to predict Gleason score ≥7 cancer on combined MRI-targeted and systematic biopsy [28]. This nomogram's AUC was 0.82 in biopsy naïve men and 0.86 in men with a prior negative biopsy.

Our nomogram is the first to provide an individual risk of csCaP at RP based solely on a combination of PSA density and mpMRI data. We found that the model had a satisfactory performance in predicting csCaP at RP (AUC 0.77) and was well calibrated in internal validation, with a better performance compared to models that do not incorporate MRI findings [26,29]. However, the performance of our nomogram was lower than those of van Leeuwen and Bjurlin, and the investigation of the net benefits of decision curve analyses was not satisfactory. This could be mainly related to the underestimation of AUC associated with the imbalanced distribution of study outcome with a very low number of patients having non-csCaP (7.6 %) compared

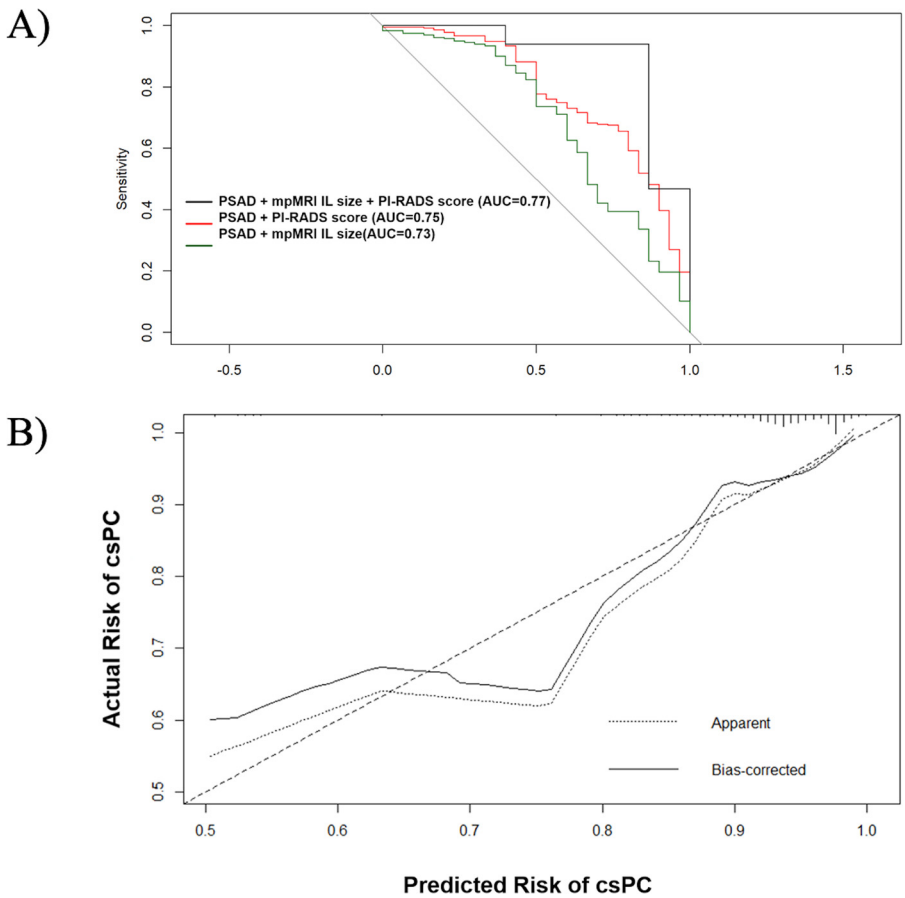

Fig. 1. (A) Receiver Operator Characteristics curve analysis showing the predictive accuracy of the full model [Prostate Imaging-Reporting and Data System (PI-RADS) score, Prostate-Specific Antigen (PSA) density, and the maximum length of the without multiparametric magnetic resonance imaging (mpMRI) index lesion (IL) size] compared to the model without PI-RADS score and mpMRI IL size. (B) The calibration plot of the full model predicting the risk of clinically significant prostate cancer.

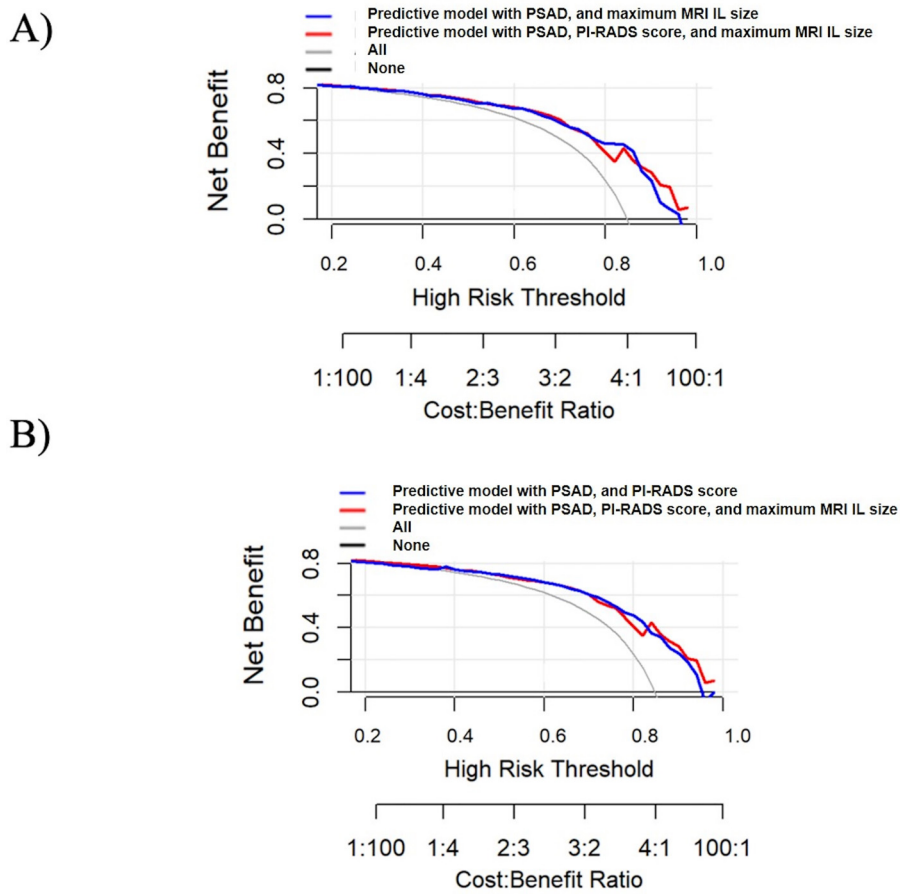

Fig. 2. The decision curve analysis shows a net benefit of multiparametric magnetic resonance imaging (mpMRI) index lesion (IL) size and Prostate Imaging-Reporting and Data System (PI-RADS) score, as shown after comparing predictive models with and without mpMRI IL size (Fig. 2A) and those with and without PI-RADS score (Fig. 2B).

with previous studies, which might have increased the risk threshold to intercept significant net benefits. Despite high thresholds (80-100%) are not clinically plausible, we think that even a small improvement in the net benefit performance for thresholds of 50-70% should be considered when dealing with populations with high csCaP prevalence.

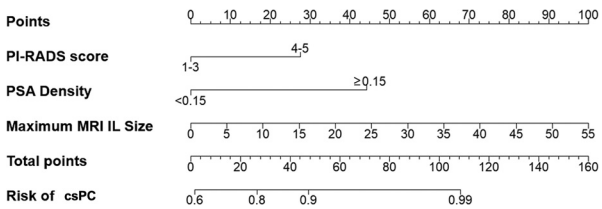

Fig. 3. Nomogram predicting the probability of clinically significant prostate cancer at radical prostatectomy. IL=Index lesion; MRI = magnetic resonance imaging; PI-RADS = Prostate Imaging-Reporting and Data System; PSA = prostate-specific antigen; csCaP= clinically significant prostate cancer. *Instructions*: locate the patient's PI-RADS score on the age axis. Draw a line straight upward to the point axis to determine how many points on the probability of significant prostate cancer the patient receives for his PI-RADS score. The same process has to be performed for each additional variable. Sum the points for each predictor. Locate the final sum on the total-point axis. Draw a line straight down to find the patient's probability of having clinically significant prostate cancer.

Additionally, the net benefit of the DCA of the model including PI-RADS score, maximum MRI IL size, and PSA density was slightly better than those excluding either IL size (Delta net benefit of 0.0111) or PI-RADS (Delta net benefit of 0.0278), and this improvement started at a 50% risk threshold. In addition, we used the whole-mount RP specimen as the reference standard instead of the biopsy needle, possibly allowing for more accurate detection of actual csCaP. Only 30 patients had non csCaP at RP as compared with 72 patients at needle biopsy, confirming that the current criteria adopted for the definition of non csCaP can miss some patients harboring csCaP. Indeed, the upgrade of the biopsy Gleason score 3+4 at RP was found to be 38.8% and 16.7% in standard biopsy and MRI/ultrasound fusion biopsy, respectively [30]. Moreover, patients with a biopsy Gleason score 6, small prostate volume, and high PSA density were found to be associated with an upgrade of the Gleason score at RP [31].

There is rising concern among urologists about the overdiagnosis of indolent CaP, given that we have witnessed an overuse of prostate biopsies in the last 3 decades, with the detection of a large number of Gleason score 6 cancers [32]. Consequently, active surveillance programs have been

developed but with increasing costs related to outpatient visits, PSA dosage, MRI and repeat biopsy, and a potentially negative impact on patients' quality of life due to complications and anxiety [33]. The inclusion of nomograms to evaluate the risk of csCaP in clinical practice might help with better patient counseling before prostate biopsy. Therefore, we believe that our nomogram might be particularly useful for counseling 2 groups of patients: i) patients undergoing a re-biopsy; ii) patients on active surveillance. Nowadays, both groups should undergo a mpMRI study before repeating biopsy and mpMRI has a central role in biopsy decision making. Interestingly, we found that only 11.3% of patients harboring csCaP had a PI-RADS score ≤3 index lesion at mpMRI, whereas a PI-RADS score ≤3 index lesion was found in 40% of men with non-csCaP. In our model, patients having a PI-RADS score 4 index lesion have at least a 70% risk of harboring csCaP at RP, whereas this risk is higher at 83% in the presence of a PI-RADS score 5 index lesion irrespective of age, PSA value, and MRI lesion size. Consequently, most patients with a previous negative biopsy and on active surveillance might avoid biopsy after negative MRI findings and a low total PSA, thus avoiding overdiagnosis of indolent CaP, given that there are 2 men diagnosed with non-csCaP for every man with csCaP detected by systematic biopsy after a negative mpMRI [32].

The present study has some limitations, starting with its retrospective nature. However, all patients were selected from our prospectively collected database. Moreover, patient selection for RP might be biased, since the study was single-center. However, MRI and RP specimens were assessed by expert specialists in their respective fields and RP specimens discovered 31 patients harboring csCaP that was categorized as non-significant on pathologic findings at needle biopsy. Finally, the prediction model requires external validation to assess its applicability, even if the usefulness of the nomogram is supported by its accurate prediction ability and internal validation.

5. Conclusion

The nomogram constructed in this study integrates mpMRI PI-RADS-v2 scoring system findings with PSA density and can assist urologists in assessing an individual's risk of csCaP. The use of a whole-mount RP specimen as the reference standard produces a more accurate detection of actual csCaP compared to needle biopsy. However, our nomogram requires external validation to confirm its prediction ability.

Author contribution statement

Daniele Castellani: Conceptualization; Data curation; Methodology; Roles/Writing − original draft; Writing − review & editing; Validation; Visualization. Sara Cecchini and Roberta Mazzucchelli: Conceptualization; Data curation; Methodology Roles/Writing − original draft. Luca Soraci, Mirko Di Rosa and Paolo Fabbietti: Methodology; Formal analysis. Erika Palagonia, Francesca Carnevali, and Francesca Puccio: Data curation; Investigation. Enrico Paci, Rodolfo Montironi and Andrea Benedetto Galosi: Investigation; Project administration; Supervision.

All authors participated in manuscript writing, review, and approval of the final version of the manuscript for submission.

Reference

[1] Sonn GA, Chang E, Natarajan S, Margolis DJ, Macairan M, Lieu P, et al. Value of targeted prostate biopsy using magnetic resonance-ultrasound fusion in men with prior negative biopsy and elevated prostate-specific antigen. Eur Urol 2014;65:809–15. https://doi.org/10.1016/j.eururo.2013.03.025.

[2] Ahmed HU, El-Shater Bosaily A, Brown LC, Gabe R, Kaplan R, Parmar MK, et al. Diagnostic accuracy of multi-parametric MRI and TRUS biopsy in prostate cancer (PROMIS): a paired validating confirmatory study. Lancet 2017;389:815–22. https://doi.org/10.1016/S0140-6736(16)32401-1.

[3] Kasivisvanathan V, Rannikko AS, Borghi M, Panebianco V, Mynderse LA, Vaarala MH, et al. MRI-targeted or standard biopsy for prostate-cancer diagnosis. N Engl J Med 2018;378:1767–77. https://doi.org/10.1056/NEJMoa1801993.

[4] Moldovan PC, Van den Broeck T, Sylvester R, Marconi L, Bellmunt J, van den Bergh RCN, et al. What is the negative predictive value of multiparametric magnetic resonance imaging in excluding prostate cancer at biopsy? A systematic review and meta-analysis from the european association of urology prostate cancer guidelines panel. Eur Urol 2017;72:250–66. https://doi.org/10.1016/j.eururo.2017.02.026.

[5] Mottet N, Vice-chair PC, Van Den Bergh RCN, Grummet J, Henry AM, Van Der Kwast TH, et al. EAU - EANM - ESTRO - ESUR - ISUP - SIOG Guidelines on Prostate Cancer 2021. https://uroweb.org/wp-content/uploads/EAU-EANM-ESTRO-ESUR-ISUP-SIOG-Guidelines-on-Prostate-Cancer-2021V4.pdf. (accessed July 4, 2021).

[6] van Leeuwen PJ, Hayen A, Thompson JE, Moses D, Shnier R, Böhm M, et al. A multiparametric magnetic resonance imaging-based risk model to determine the risk of significant prostate cancer prior to biopsy. BJU Int 2017;120:774–81. https://doi.org/10.1111/bju.13814.

[7] Mehralivand S, Shih JH, Rais-Bahrami S, Oto A, Bednarova S, Nix JW, et al. A magnetic resonance imaging-based prediction model for prostate biopsy risk stratification. JAMA Oncol 2018;4:678–85. https://doi.org/10.1001/jamaoncol.2017.5667.

[8] Dwivedi DK, Kumar R, Dwivedi AK, Bora GS, Thulkar S, Sharma S, et al. Prebiopsy multiparametric MRI-based risk score for predicting prostate cancer in biopsy-naive men with prostate-specific antigen between 4-10 ng/mL. J Magn Reson Imaging 2018;47:1227–36. https://doi.org/10.1002/jmri.25850.

[9] Alberts AR, Roobol MJ, Verbeek JFM, Schoots IG, Chiu PK, Osses DF, et al. Prediction of high-grade prostate cancer following multiparametric magnetic resonance imaging: improving the rotterdam european randomized study of screening for prostate cancer risk calculators. Eur Urol 2019;75:310–8. https://doi.org/10.1016/j.eururo.2018.07.031.

[10] Barentsz JO, Weinreb JC, Verma S, Thoeny HC, Tempany CM, Shtern F, et al. Synopsis of the PI-RADS v2 guidelines for multiparametric prostate magnetic resonance imaging and recommendations for use. Eur Urol 2016;69:41–9. https://doi.org/10.1016/j.eururo.2015.08.038.

[11] Montironi R, Mazzucchelli R, Kwast T. Morphological assessment of radical prostatectomy specimens. A protocol with clinical relevance.

Virchows Arch 2003;442:211–7. https://doi.org/10.1007/s00428-002-0741-7.

[12] Montironi R, Lopez Beltran A, Mazzucchelli R, Cheng L, Scarpelli M. Handling of radical prostatectomy specimens: total embedding with large-format histology. Int J Breast Cancer 2012;2012:932784. https://doi.org/10.1155/2012/932784.

[13] Montironi R, Lopez-Beltran A, Mazzucchelli R, Scarpelli M, Bollito E. Assessment of radical prostatectomy specimens and diagnostic reporting of pathological findings. Pathologica 2001;93:226–32.

[14] Epstein JI, Egevad L, Amin MB, Delahunt B, Srigley JR, Humphrey PA. The 2014 international society of urological pathology (ISUP) consensus conference on gleason grading of prostatic carcinoma definition of grading patterns and proposal for a new grading system. Am J Surg Pathol 2016;40:244–52. https://doi.org/10.1097/PAS.0000000000000530.

[15] Epstein JI, Walsh PC, Carmichael M, Brendler CB. Pathologic and clinical findings to predict tumor extent of nonpalpable (stage T1c) prostate cancer. JAMA 1994;271:368–74.

[16] Stamey TA, McNeal JM, Wise AM, Clayton JL. Secondary cancers in the prostate do not determine PSA biochemical failure in untreated men undergoing radical retropubic prostatectomy. Eur Urol 2001;39 (Suppl 4):22–3. https://doi.org/10.1159/000052577.

[17] Miles J. Tolerance and variance inflation factor. Wiley StatsRef Stat Ref Online, (Hoboken, New Jersey, USA); 2014. https://doi.org/10.1002/9781118445112.stat06593.

[18] Bozdogan H. Model selection and Akaike's Information Criterion (AIC): the general theory and its analytical extensions. Psychometrika 1987;52:345–70. https://doi.org/10.1007/BF02294361.

[19] Harrell FEJ, Lee KL, Mark DB. Multivariable prognostic models: issues in developing models, evaluating assumptions and adequacy, and measuring and reducing errors. Stat Med 1996;15:361–87. https://doi.org/10.1002/(SICI)1097-0258(19960229)15:4<361::AID-SIM168>3.0.CO;2-4.

[20] Royston P. Model selection for univariable fractional polynomials. Stata J 2017;17:619–29.

[21] Vickers AJ, Elkin EB. Decision curve analysis: a novel method for evaluating prediction models. Med Decis Mak an Int J Soc Med Decis Mak 2006;26:565–74. https://doi.org/10.1177/0272989X06295361.

[22] Robin X, Turck N, Hainard A, Tiberti N, Lisacek F, Sanchez J-C, et al. pROC: an open-source package for R and S+ to analyze and compare ROC curves. BMC Bioinformatics 2011;12:77. https://doi.org/10.1186/1471-2105-12-77.

[23] Brown M. rmda: risk model decision analysis. https://mdbrown.github.io/rmda/. accessed January 7, 2021.

[24] Matoso A, Epstein JI. Defining clinically significant prostate cancer on the basis of pathological findings. Histopathology 2019;74:135–45. https://doi.org/10.1111/his.13712.

[25] Roobol MJ, Steyerberg EW, Kranse R, Wolters T, van den Bergh RCN, Bangma CH, et al. A risk-based strategy improves prostate-specific antigen-driven detection of prostate cancer. Eur Urol 2010;57:79–85. https://doi.org/10.1016/j.eururo.2009.08.025.

[26] Thompson IM, Ankerst DP, Chi C, Goodman PJ, Tangen CM, Lucia MS, et al. Assessing prostate cancer risk: results from the Prostate Cancer Prevention Trial. J Natl Cancer Inst 2006;98:529–34. https://doi.org/10.1093/jnci/djj131.

[27] Hamoen EHJ, de Rooij M, Witjes JA, Barentsz JO, Rovers MM. Use of the Prostate Imaging Reporting and Data System (PI-RADS) for prostate cancer detection with multiparametric magnetic resonance imaging: a diagnostic meta-analysis. Eur Urol 2015;67:1112–21. https://doi.org/10.1016/j.eururo.2014.10.033.

[28] Bjurlin MA, Rosenkrantz AB, Sarkar S, Lepor H, Huang WC, Huang R, et al. Prediction of prostate cancer risk among men undergoing combined MRI-targeted and Systematic biopsy using novel pre-biopsy nomograms that incorporate MRI findings. Urology 2018;112:112–20. https://doi.org/10.1016/j.urology.2017.09.035.

[29] Kranse R, Roobol M, Schröder FH. A graphical device to represent the outcomes of a logistic regression analysis. Prostate 2008;68:1674–80. https://doi.org/10.1002/pros.20840.

[30] De Luca S, Fiori C, Bollito E, Garrou D, Aimar R, Cattaneo G, et al. Risk of Gleason Score 3+4=7 prostate cancer upgrading at radical prostatectomy is significantly reduced by targeted versus standard biopsy. Minerva Urol Nefrol 2020;72:360–8. https://doi.org/10.23736/S0393-2249.19.03367-8.

[31] Pourmand G, Gooran S, Hossieni SR, Guitynavard F, Safavi M, Sharifi A, et al. Correlation of preoperative and radical prostatectomy gleason score: examining the predictors of upgrade and downgrade results. Acta Med Iran 2017;55:249–53.

[32] Drost F-JH, Osses DF, Nieboer D, Steyerberg EW, Bangma CH, Roobol MJ, et al. Prostate MRI, with or without MRI-targeted biopsy, and systematic biopsy for detecting prostate cancer. Cochrane Database Syst Rev 2019;4:CD012663. https://doi.org/10.1002/14651858.CD012663.pub2.

[33] Keegan KA, Dall'Era MA, Durbin-Johnson B, Evans CP. Active surveillance for prostate cancer compared with immediate treatment: an economic analysis. Cancer 2012;118:3512–8. https://doi.org/10.1002/cncr.26688.